JOC Article

An Orifice-Size Index for Open-Cage Fullerenes†

Shih-Ching Chuang,‡ Yasujiro Murata,*,‡,§ Michihisa Murata,‡ and Koichi Komatsu*,‡,||

Institute for Chemical Research, Kyoto University, Uji, Kyoto 611-0011, Japan, PRESTO, Japan Science and Technology Agency, and Department of Environmental and Biotechnological Frontier Engineering, Fukui University of Technology, Gakuen, Fukui 910-8505, Japan

yasujiro@scl.kyoto-u.ac.jp; komatsu@scl.kyoto-u.ac.jp

Received April 16, 2007

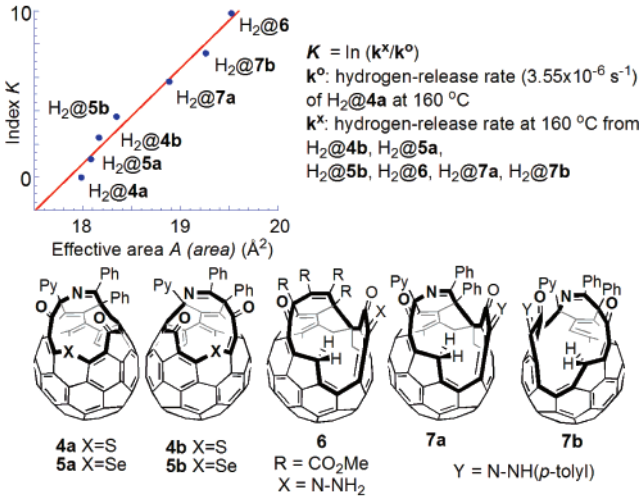

In the field of open-cage fullerenes, there was a lack of a universal standard that could correlate and quantify the orifice size of open-cage fullerenes. One cannot compare the relative orifice size by simple comparison of the number of atoms that composes the orifice. We present a general term for easy estimation of relative orifice size by defining an index for open-cage fullerenes. We estimated the corresponding effective areas *A(area)* for orifices of open-cage fullerenes by matching calculated activation energies *Ea(calcd)* for hydrogen release from open-cage fullerenes (B3LYP/6-31G**//B3LYP/3-21G) to the computed energies required for a hydrogen molecule passing through a cyclo[*n*]carbon ring. Then we define an index *K(orifice)* based on experimental hydrogen release rate, where *K(orifice)* = ln *k*/*k*° (*k* is rate constant of hydrogen-release rate of any open-cage fullerenes taken for comparison at 160 °C; *k*° is the hydrogen release rate from H_2@**4a** taken as the standard compound). We synthesized several open-cage fullerenes and studied kinetics of a set of H_2-encapsulated open-cage fullerenes to evaluate their *K* values. A correlation of the index *K(orifice)* with the effective areas *A(area)* showed a good linear fit (r^2 = 0.972) that demonstrated a good interplay between experiment and theory. This allows one to estimate *K(orifice)* index and/or relative rate *k* of hydrogen release through computing activation energy *Ea-(calcd)* for a designed open-cage fullerene.

Introduction

Recently, the endohedral complexes of open-cage fullerenes[1] have drawn significant attention since the preparation of H_2@C_{60} has been achieved synthetically through the route of opening and closure of an orifice on C_{60} cage.[2] The ultimate purpose for the creation of an orifice on the fullerene cage is the substitution of conventional approach for preparation of entirely new endohedral fullerenes and elucidation of their physical and chemical properties.[3] Because the encapsulated species of reported endohedral open-cage fullerene complexes are confined to neutral and small atom and molecules such as He,[1f,k,n] H_2,[1f,j,2b]

† This paper is dedicated to the memory of Professor Yoshihiko Ito.
‡ Kyoto University.
§ Japan Science and Technology Agency.
|| Fukui University of Technology.

10.1021/jo070790w CCC: $37.00
Published on Web 07/19/2007

H_2O,[1h] and CO,[1l] enlargement of the orifice size for larger species and metal ions of considerable size is an ongoing desire. In this regime, there has been a lack of a universal standard that could quantify the orifice size of open-cage fullerenes. One cannot compare the relative orifice size by simple comparison of the number of atoms that composes a ring. A clear example has been shown from the contradiction that an open-cage fullerene **1** having a 14-member-ring orifice[1e] required more harsh conditions than a compound having a 13-membered-ring orifice[2b] for hydrogen insertion (compound **4a** shown below).

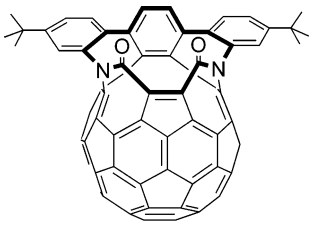

1

In this paper, we present a general term for easy estimation of relative orifice size by defining an index *K(orifice*) for open-cage fullerenes. We estimated the corresponding effective areas *A(area*) for orifices of open-cage fullerenes by matching calculated activation energies *Ea(calcd*) for hydrogen release to calculated energies required for a hydrogen molecule to pass through a imaginary cyclo[*n*]carbon ring whose enclosing areas could be easily computed.[4] We established a good linear correlation between the index *K(orifice*) and the effective areas *A(area*) for orifices of several open-cage fullerenes. This will allow one to approximate *real hydrogen release rate* and *activation energies* simply by calculation.

To achieve our purpose for indexing orifice sizes, some open-cage fullerenes with similar opening patterns are desired. Our approach for expanding the orifice takes advantages of our previous synthetic method by inserting group 16 elements into the rim of the orifice of compound **3a**.[2a,1m] In our previous study, the other isomer, compound **3b**, obtained as a minor product together with **3a** upon photochemical oxidation of **2**, has not been utilized due to its lower yield.[2a] Their corresponding 13-membered-ring compounds encapsulating molecular hydrogen, H_2@**4b** and H_2@**5b**, displayed faster rates of hydrogen release than H_2@**4a** and H_2@**5a**. These four structurally similar 13-membered-ring compounds have thus triggered our investigation of their relative opening sizes.

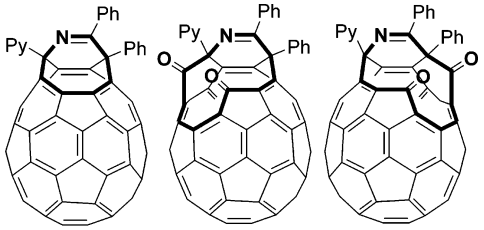

2 **3a** **3b**

Py = 2-pyridyl

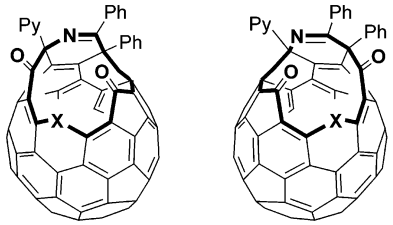

4a X=S
5a X=Se

4b X=S
5b X=Se

Results and Discussion

Open-cage fullerenes **4b** and **5b** were synthesized by a modified method based on previous study, i.e., two-electron reduction of the precursor **3b** followed by reaction with elemental sulfur or selenium.[1m,2a,5] Their corresponding H_2-encapsulating compounds, H_2**@4a**,**b** and H_2**@5a**,**b**, were prepared under high pressure of hydrogen (see Experimental Section). We studied first-order hydrogen release rates *k* at various temperatures for all four compounds, H_2@**4a**, H_2@**4b**, H_2@**5a**, and H_2@**5b**, by monitoring their ^{1}H NMR at 130−190 °C in *o*-dichlorobenzene-d_4. The integrated peak area of a sharp singlet signal around −7 ppm of encapsulated hydrogen molecule relative to that of a proton signal of 2-pyridyl group was used to determine the encapsulation ratio of hydrogen at suitable time intervals. As summarized in Table 1, the rates of hydrogen-release for all four compounds at 160 °C were determined as $3.55 \pm 0.03 \times 10^{-6}$, $1.05 \pm 0.04 \times 10^{-5}$, $3.90 \pm 0.09 \times 10^{-5}$, and $1.35 \pm 0.03 \times 10^{-4}$ s^{-1} for H_2@**4a**,[2b] H_2@**5a**[1m], H_2@**4b**, and H_2@**5b**, respectively, which indicated their orifice-size order of **5b** > **4b** > **5a** > **4a**. It is to be noted that compound **4b** has a larger opening size than that of compound **5a** despite that compound **5a** has a Se atom, which is larger than S, in the rim of the orifice.

Recently, Iwamatsu et al. reported open-cage fullerene complex H_2@**6**[1i,6] with a 16-membered-ring orifice encapsulating hydrogen molecule and investigated its hydrogen release

(1) (a) Arce, M.-J.; Viado, A. L.; An, Y.-Z.; Khan, S. I.; Rubin, Y. *J. Am. Chem. Soc.* **1996**, *118*, 3775−3776. (b) Rubin, Y. *Chem.−Eur. J.* **1997**, *3*, 1009−1016. (c) Rubin, Y. *Chimia* **1998**, *52*, 118−126. (d) Rubin, Y. *Top. Curr. Chem.* **1999**, *199*, 67−91. (e) Schick, G.; Jarrosson, T.; Rubin, Y. *Angew. Chem., Int. Ed.* **1999**, *38*, 2360−2363. (f) Rubin, Y.; Jarrosson, T.; Wang, G.-W.; Bartberger, M. D.; Houk, K. N.; Schick, G.; Saunders, M.; Cross, R. J. *Angew. Chem., Int. Ed.* **2001**, *40*, 1543−1546. (g) Nierengarten, J.-F. *Angew. Chem., Int. Ed.* **2001**, *40*, 2973−2974. (h) Iwamatsu, S.; Uozaki, T.; Kobayashi, K.; Re, S.; Nagase, S.; Murata, S. *J. Am. Chem. Soc.* **2004**, *126*, 2668−2669. (i) Iwamatsu, S.; Murata, S.; Andoh, Y.; Minoura, M.; Kobayashi, K.; Mizorogi, N.; Nagase, S. *J. Org. Chem.* **2005**, *70*, 4820−4825. (j) Iwamatsu, S.; Murata, S. *Synlett* **2005**, *14*, 2117−2129. (k) Stanisky, C. M.; Cross, R. J.; Saunders, M.; Murata, M.; Murata, Y.; Komatsu, K. *J. Am. Chem. Soc.* **2005**, *127*, 299−302. (l) Iwamatsu, S.; Stanisky, C. M.; Cross, R. J.; Saunders, M.; Mizorogi, N.; Nagase, S.; Murata, S. *Angew. Chem., Int. Ed.* **2006**, *45*, 5337−5340. (m) Chuang, S.-C.; Murata, Y.; Murata, M.; Mori, S.; Maeda, S.; Tanabe, F.; Komatsu, K. *Chem. Commun.* **2007**, 1278−1280. (n) Chuang, S.-C.; Murata, Y.; Murata, M.; Komatsu, K. *Chem. Commun.* **2007**, 1751−1753.

(2) (a) Murata, Y.; Murata, M.; Komatsu, K. *Chem.−Eur. J.* **2003**, *9*, 1600−1609. (b) Murata, Y.; Murata, M.; Komatsu, K. *J. Am. Chem. Soc.* **2003**, *125*, 7152−7153. (c) Komatsu, K.; Murata, M.; Murata, Y. *Science* **2005**, *307*, 238−240. (d) Komatsu, K.; Murata, Y. *Chem. Lett.* **2005**, *34*, 886−891. (e) Murata, M.; Murata, Y.; Komatsu, K. *J. Am. Chem. Soc.* **2006**, *128*, 8024−8033.

(3) (a) Saunders, M.; Jiménez-Vázquez, H. A.; Cross, R. J.; Mroczkowski, S.; Freedberg, D. I.; Anet, F. A. L. *Nature* **1994**, *367*, 256−258. (b) Kobayashi, S.; Mori, S.; Iida, S.; Ando, H.; Takenobu, T.; Taguchi, Y.; Fujiwara, A.; Taninaka, A.; Shinohara, H.; Iwasa, Y. *J. Am. Chem. Soc.* **2003**, *125*, 8116−8117. (c) *Endofullerenes: A New Family of Carbon Clusters*; Akasaka, T., Nagase, S., Eds.; Kluwer Academic Publishers: Dodrecht, The Netherlands, 2002.

(4) Diederich, F.; Rubin, Y.; Knobler, C. B.; Whetten, R. L.; Schriver, K. E.; Houk, K. N.; Li, Y. *Science* **1989**, *245*, 1088−1090.

(5) See Experimental Section for the synthesis of new compounds **4b**, **5b**, H_2**@4b**, and H_2**@5b** and Supporting Information for their spectral data. Compound **4a**, **5a**, and their corresponding hydrogen encapsulated species H_2**@4a** and H_2**@5a** were reported previously (see ref 1m and 2a).

(6) Compound **6** corresponds to compound **3c** in reference 1i.

TABLE 1. First-Order Rate Constants k ($\times 10^{-6}$, s^{-1}) for Hydrogen Release from Compounds H_2@4a,[2b] H_2@4b, H_2@5a,[1m] and H_2@5b at Various Temperatures

	temp (°C)						
compd	130	140	150	160	170	180	190
H_2@**4a**[a]				3.55 ± 0.03[a]	9.10 ± 0.05[a]	21.3 ± 0.2[a]	45.3 ± 0.9[a]
H_2@**5a**[b]			4.63 ± 0.27[b]	10.5 ± 0.04[b]	26.2 ± 0.4[b]	57.2 ± 4.8[b]	
H_2@**4b**	2.60 ± 0.08	6.63 ± 0.02	16.1 ± 0.7	39.0 ± 0.9			
H_2@**5b**	10.7 ± 0.4	24.5 ± 1.7	55.4 ± 4.0	135 ± 3			

[a] Values and errors in the previous study were recalculated; see ref 1m. [b] Values taken from ref 1m.

TABLE 2. First-Order Rate Constants k ($\times 10^{-6}$, s^{-1}) for Hydrogen Release from Compounds H_2@6,[1i] H_2@7a, and H_2@7b at Various Temperatures

	temp (°C)						
compd	70	80	90	100	110	120	160[b]
H_2@**6**[a]	95 ± 16[a]	250 ± 10[a]	540 ± 40[a]	1250 ± 90 [a]			70500[b]
H_2@**7a**			1.47 ± 0.08	4.05 ± 0.33	12.4 ± 0.6	33.5 ± 2.8	1120[b]
H_2@**7b**		4.62 ± 0.20	15.4 ± 1.1	45.6 ± 3.3	93.1 ± 0.6		6440[b]

[a] Values taken from ref 1i. [b] Extrapolated values from Arrhenius plots.

TABLE 3. Kinetic and Thermodynamic Data (25 °C) for Hydrogen Release of Compounds H_2@4a, H_2@4b, H_2@5a, H_2@5b, H_2@6, H_2@7a, and H_2@7b

compd	$t_{1/2}$[c]	*Ea*(*exp*)[e]	A	$\Delta G^{\ddagger}$[e]	$\Delta H^{\ddagger}$[e]	$\Delta S^{\ddagger}$[f]	*Ea*(*calcd*)[g]
H_2@**4a**[a]	53.9[a]	34.2 ± 0.6[a]	$10^{11.8 \pm 0.3}$[a]	35.6 ± 0.6[a]	33.4 ± 0.6[a]	-7.5 ± 1.3[a]	28.9[a]
H_2@**5a**[a]	18.3[a]	32.4 ± 0.7[a]	$10^{11.3 \pm 0.3}$[a]	34.4 ± 0.7[a]	31.5 ± 0.7[a]	-9.6 ± 1.5[a]	28.2[a]
H_2@**4b**	4.94	31.4 ± 0.2	$10^{11.4 \pm 0.1}$	33.3 ± 0.2	30.6 ± 0.2	-9.2 ± 0.5	27.6
H_2@**5b**	1.43	29.3 ± 0.8	$10^{10.9 \pm 0.4}$	32.0 ± 0.8	28.5 ± 0.8	-11.6 ± 1.9	26.4
H_2@**6**[b]	0.00273[d]	21.7 ± 0.4[b]	$10^{9.8 \pm 0.3}$[b]	25.8 ± 0.8 [b]	21.0 ± 0.4[b]	-15.9 ± 1.2[b]	19.8[b]
H_2@**7a**	0.172[d]	29.9 ± 0.6	$10^{12.1 \pm 0.4}$	30.9 ± 0.6	29.2 ± 0.6	-5.7 ± 1.6	23.1
H_2@**7b**	0.0299[d]	27.3 ± 1.7	$10^{11.6 \pm 1.0}$	29.1 ± 1.7	26.7 ± 1.7	-7.9 ± 4.7	21.1

[a] Values taken from ref 1m. [b] Values taken from ref 1i. [c] Half-lives (h) at 160 °C determined experimentally. [d] Half-lives (h) at 160 °C extrapolated from Arrhenius plots. [e] Unit in kcal mol^{-1}. [f] Unit in cal K^{-1} mol^{-1}. [g] Calculated activation energy at B3LYP/6-31G**//B3LYP/3-21G level of theory, in kcal mol^{-1}.

rates at 70−100 °C, as shown in Table 2. By applying Iwamatsu's method to our compounds **3a** and **3b**, we synthesized compounds H_2@**7a** and H_2@**7b**, respectively, and studied their kinetics of hydrogen releases (Table 2).

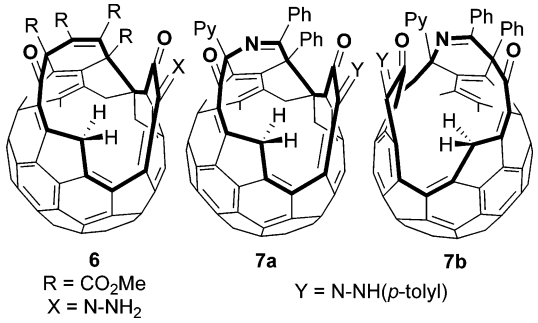

6 **7a** **7b**

R = CO_2Me
X = N-NH_2

Y = N-NH(*p*-tolyl)

Based on the hydrogen release rates k at studied temperatures and Arrhenius plots, we obtained kinetic and thermodynamic data summarized in Table 3. The activation barriers *Ea*(*exp*) for hydrogen release showed the order of the ease of hydrogen release and were in a relatively good agreement with the computed barriers *Ea*(*calcd*) at the B3LYP/6-31G**//B3LYP/3-21G level of theory.[7] The calculated distances between two carbonyl carbons (B3LYP/3-21G*), 3.75, 3.79, 3.89, and 3.97 Å for **4a**, **5a**, **4b**, and **5b**, respectively, are reflected in the order of orifice sizes. Interestingly, among 13-membered-ring systems, the $\Delta S^{\ddagger}$ values followed such an order of H_2@**4a** > H_2@**4b** > H_2@**5a** > H_2@**5b**, which is considered to reflect the relative cage size. Larger cage would allow encapsulated hydrogen to own more motional degrees of freedom in the ground state and hence to lose degrees of freedom to a larger extent at the transition state, exhibiting more negative value of $\Delta S^{\ddagger}$. The similar trend is also observed for the 16-membered-ring system, in which the order of $\Delta S^{\ddagger}$ is H_2@**7a** > H_2@**7b** > H_2@**6**.

To categorize these open-cage fullerenes, we defined the hydrogen index *K*(*orifice*) to quantify the relative orifice size by taking the first-order rate constant of hydrogen release from H_2@**4a** at 160 °C as the standard reference $k°$ (3.55×10^{-6} s^{-1}). Thus *K*(*orifice*) = ln $k/k°$ can be used to stand for the relative orifice size, where k is the rate constant of hydrogen release at 160 °C from any open-cage fullerenes. The larger the value of *K*(*orifice*) is, the larger the size of an orifice of open-cage fullerene is. The K values thus determined for compound H_2@**4a**, H_2@**5a**, H_2@**4b**, and H_2@**5b** are 0.00, 1.08, 2.40, and 3.64, respectively (Table 4). A value of *K*(*orifice*) can be assigned to any newly discovered open-cage fullerenes as long as the hydrogen-release rate at 160 °C could be measured or extrapolated by Arrhenius plot. We chose rate constant of hydrogen release to define this index rather than that of ^{3}He because of common availability of hydrogen and also an NMR probe for ^{1}H than ^{3}He.[8] A negative value of index *K*(*orifice*) indicates the size of orifice is too small for hydrogen insertion and thus requires more harsh conditions for insertion of

(7) See Supporting Information for optimized structures, single point energies, and full citation of GAUSSIAN 03 software.

(8) For examples, see ref 1f and 1k.

TABLE 4. The Hydrogen-Release Index *K*(*orifice*) and the Effective Area *A*(*area*) for Orifices of Open-Cage Fullerenes H_2@4a**−**b**, H_2@**5a**−**b**, H_2@**6**, and H_2@**7a**−**b**

compd	*K*(*orifice*)[a]	*A*(*area*)[b]
H_2@**4a**	0.00	17.98
H_2@**5a**	1.08	18.08
H_2@**4b**	2.40	18.16
H_2@**5b**	3.64	18.34
H_2@**6**	9.90	19.52
H_2@**7a**	5.76	18.88
H_2@**7b**	7.50	19.26

[a] Defined by ln $k/k°$, where k is the rate constant of hydrogen release at 160 °C and $k°$ is that of H_2@**4a**. [b] Obtained by eq 1 using calculated activation energy *Ea*(*calcd*) at the B3LYP/6-31G**//B3LYP/3-21G level of theory, in Å^2.

hydrogen than that carried out for compound **4a**. The hydrogen insertion into compound **4a** was practically carried out at a pressure of 800 atm of hydrogen gas at 200 °C for 8 h.[2b]

From its definition, the index *K*(*orifice*) should be correlated with the area of orifice. However, it is not simple to define the area of an orifice since the atoms present at the rim of orifice are generally not in the same plane and the orifice is influenced by the presence of substituents. Particularly, the van der Waals interactive friction between H_2 and surrounding atoms at the transition state cannot be evaluated from the calculated transition-state structure. These complex factors make estimation of the *real* area of an opening difficult. Hence, in order to estimate the *effective* area *A*(*area*) of the orifice of open-cage fullerenes with irregular shape, we investigated the correlation of activation energies for hydrogen passage through *imaginary* cyclo[*n*]carbons (n = 10, 12, 14, 16, 18) as an ideal ring system, at the same level of theory (B3LYP/6-31G**//B3LYP/3-21G). We computed transition-state structures of H_2 to pass through cyclo[*n*]carbons (Figure 1) and their corresponding single point energies. A nonlinear correlation of the calculated activation energy *Ea*(*calcd*) with the enclosing area *A*(*area*) was best described by eq 1 (r^2 = 0.9999) for $n \geq 10$. The enclosing areas *A*(*area*) of cyclo[*n*]carbons were estimated through πr^2, where r is the calculated radius of cyclo[*n*]carbons (the distances between the center of cyclo[*n*]cabons and the carbon atoms). Based on this curve (Figure 2), the effective area *A*(*area*) of the orifice of open-cage fullerenes could be estimated by matching the computed activation energy *Ea*(*calcd*) using eq 1. Interestingly, the computed activation energies for H_2@**4a**, H_2@**4b**, H_2@**5a**, and H_2@**5b** with 13-membered-ring orifices are located between the energies corresponding to hydrogen passage through cyclo[10]carbon and cyclo[12]carbon and closer to the energies of cyclo[12]carbon. Their computed effective areas of orifices are 17.98, 18.08, 18.16, and 18.34 Å^2 based on eq 1, respectively (Table 4).

$$Ea(calc) = 1.8437 \times 10^7/A(area)^{4.6256} \quad (1)$$

In Figure 3, we show the correlation of the index *K*(*orifice*) with effective areas *A*(*area*) for orifices of open-cage fullerenes obtained by eq 1. To extend this correlation to 16-membered-ring open-cage system, the rate constants at 160 °C for H_2@**6**, H_2@**7a**−**b** were obtained by extrapolation (Table 2). Their *K*(*orifice*) indexes were obtained as 9.90, 5.76, and 7.50 for H_2@**6**, H_2@**7a**, and H_2@**7b**, respectively (Table 4). An overall linear correlation for all compounds H_2@**4a**,**b**, H_2@**5a**,**b**, H_2@**6**, and H_2@**7a**,**b** gave a linear regression (eq 2) as good as r^2 = 0.972, supporting that this correlation can be used for a wide range of open-cage fullerene systems. On the basis of this correlation, we could estimate the effective area *A*(*area*) and *K*(*orifice*) as 16.77 Å^2 and −6.16, respectively, for H_2@**1** by eq 1 and eq 2, whose experimental hydrogen-escaping rate was unavailable.

$$K(orifice) = -102.08 + 5.7198*A(area) \quad (2)$$

Another correlation of the index *K*(*orifice*) *versus* the calculated activation energy *Ea*(*calcd*) gave a linear correlation with r^2 = 0.975 (Figure 4). This plot, a reflected plot of the index *K*(*orifice*) *versus* the effective area *A*(*area*) (Figure 3), could be used to directly estimate index *K*(*orifice*) from the calculated activation energy for hydrogen release from open-cage fullerenes. In contrast, the correlation was poor (r^2 = 0.887)[9] when *K*(*orifice*) was plotted against rough estimation of the orifice area based on perimeter calculated by summation of all bond lengths of the rim. In addition, a correlation between *Ea*(*exp*) and *Ea*(*calcd*) gave only a correlation with r^2 = 0.809 (see Supporting Information).

In summary, we have provided a scope for correlating the orifice size of open-cage fullerenes with their rate constants of hydrogen release. An index *K*(*orifice*) was presented as the universal standard to quantify relative size of opening based on hydrogen-release rate constant k. We used the energies *Ea*(*calcd*) of hydrogen passing through cyclo[*n*]carbons to quantify the effective opening areas *A*(*area*) for open-cage fullerenes. The fair linear correlation of *K*(*orifice*) and effective areas *A*(*area*) for open-cage fullerenes demonstrated that experimental kinetic results were in good agreement with theory at B3LYP/6-31G**//B3LYP/3-21G level. One can estimate index *K*(*orifice*), experimental hydrogen-release rate k, and activation energy *Ea*(*exp*) for an open-cage fullerene through computing activation energy *Ea*(*calcd*) for a designed open-cage fullerene. In general, this correlation approach could be applicable to molecular containers besides open-cage fullerenes.[9]

Experimental Section

General Method. All reactions were performed under argon. Dry 1,2-dichlorobenzene (ODCB) was distilled from CaH_2 under argon. Sodium 2-methyl-2-propanethiolate (90%), sodium methylthiolate (95%), anhydrous benzonitrile, and selenium powder (100 mesh) were used as received.

Synthesis of Compound 4b. To a solution of **3b** (1.51 g, 1.45 mmol) and S_8 (376 mg, 1.45 mmol) in 100 mL dry benzonitrile at ambient temperature was added 2.2 equiv of 90% sodium 2-methyl-2-propanethiolate (396 mg, 3.51 mmol). The color of the resulting mixture turned from brown to black immediately. After stirring for 3 h, the reaction mixture was worked up by addition of I_2 (1.1 equiv, 404 mg in 20 mL of benzonitrile) and then washed with 30 mL of sat. sodium thiosulfite solution. After the organic layer was separated from aqueous layer and dried with $MgSO_4$, the organic solution was evaporated under reduced pressure. The resulting solids were redissolved in CS_2 and were subjected to column chromatography over silica gel to afford 1.17 g of **4b**. Yield: 75%. The spectral data of **4b** were identical to those of the product obtained by the use of TDAE.[2a] ^{1}H NMR (ODCB-d_4, 300 MHz) 6.87−6.93 (m, 1H), 7.24−7.38 (m, 6H), 7.50−7.56 (m, 1H), 7.79−7.82 (m,

(9) (a) Izatt, R. M.; Bradshaw, J. S.; Pawlak, K.; Bruening, R. L.; Tarbet, B. J. *Chem. Rev.* **1992**, *92*, 1261−1354. (b) Cram, D. J; Cram, J. M. *Container Molecules and Their Guests*, 1st Ed.; Royal Society of Chemistry: Cambridge, 1994. (c) Schmidtchen, F. P.; Berger, M. *Chem. Rev.* **1997**, *97*, 1609−1646. (d) Hapiot, F.; Tilloy, S.; Monflier, E. *Chem. Rev.* **2006**, *106*, 767−781.

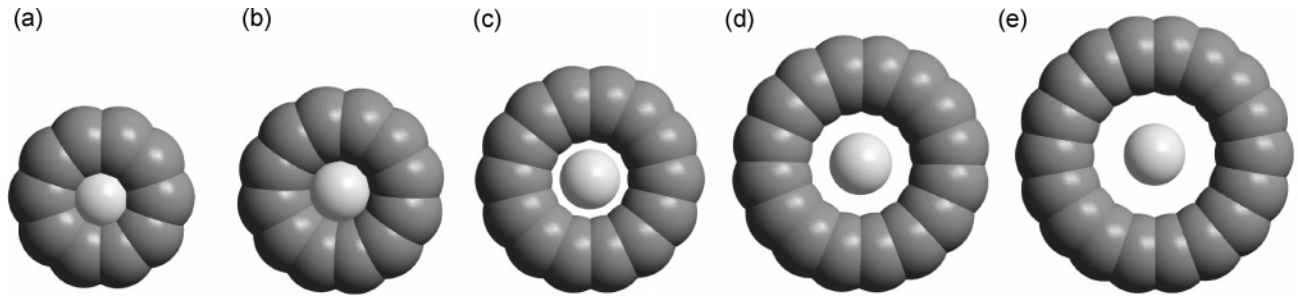

FIGURE 1. Transition-state structure for the hydrogen passage; (a) H_2-cyclo[10]carbon, (b) H_2-cyclo[12]carbon, (c) H_2-cyclo[14]carbon, (d) H_2-cyclo[16]carbon, and (e) H_2-cyclo[18]carbon, calculated at the B3LYP/3-21G level of theory.

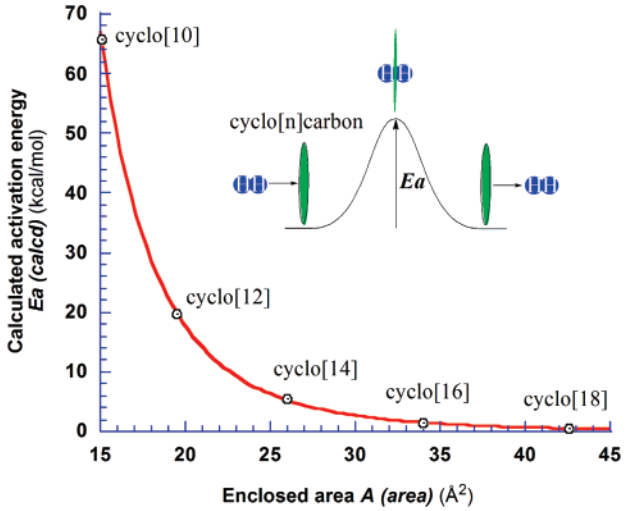

FIGURE 2. Correlation diagram of the calculated activation energy *Ea*(*calcd*) for hydrogen passage through cyclo[*n*]carbons (n = 10, 12, 14, 16, 18) (B3LYP/6-31G**//B3LYP/3-21G) with their enclosed areas *A*(*area*) defined by πr^2, where r is the radius of cyclo[*n*]carbons.

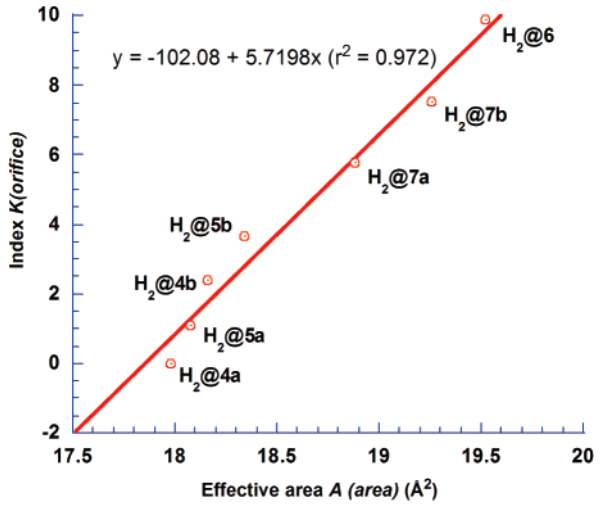

FIGURE 3. A plot of the hydrogen index *K*(*orifice*) *versus* the corresponding effective area *A*(*area*) for compounds H_2@**4a**,**b**, H_2@**5a**,**b**, H_2@**6**, and H_2@**7a**,**b**.

3H), 8.35−8.37 (m, 1H), 8.66−8.69 (m, 2H); ^{13}C NMR (ODCB-d_4, 75 MHz) δ 60.47, 72.67, 122.41, 124.88, (126.61−132.56), 132.84, 133.75, 135.30, 135.47, 136.00, 136.24, 136.75, 136.91, 137.72, 137.93, 138.04, 138.17, 138.22, 138.39, 138.57, 138.79, 139.62, 139.80, 140.20, 140.52, 140.57, 140.99, 141.23, 141.37, 141.63, 141.78, 142.76, 144.08, 145.72, 146.04, 146.32, 146.51,

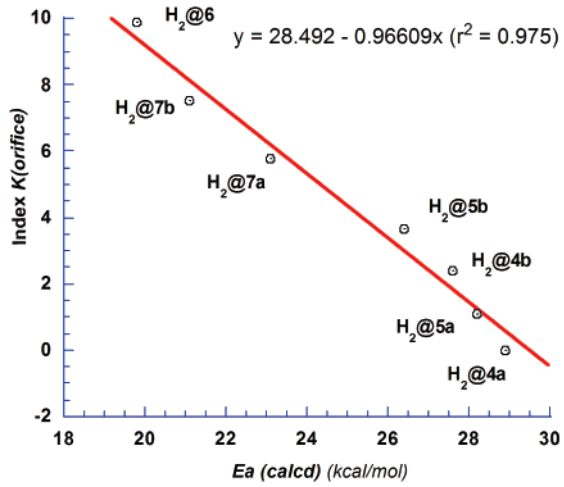

FIGURE 4. A plot of the hydrogen index *K*(*orifice*) *versus* calculated activation energy *Ea*(*calcd*) for hydrogen release from compounds H_2@**4a**−**b**, H_2@**5a**−**b**, H_2@**6**, and H_2@**7a**−**b** at the B3LYP/6-31G**//B3LYP/3-21G level of theory.

146.68, 146.74, 147.18, 147.29, 147.31, 148.34, 147.42, 147.51, 147.65, 147.87, 148.31, 148.55, 148.67, 149.34, 149.39, 150.09, 151.30, 159.15, 166.08, 185.88, 192.59; FT-IR ν (cm^{-1}) (C═O) 1697, 1746. UV−vis ($CHCl_3$, 5.66 × 10^{-5} M) $\lambda_{max}(\epsilon)$ 222 (1.40 × 10^4), 258 (1.41 × 10^4), 318 (5.04 × 10^3), 426 (6.51 × 10^2). HR-FAB MS calcd for $C_{80}H_{15}O_2N_2S$ (M + H$^+$): 1067.0854; found: 1067.0852.

Synthesis of Compound 5b. A solution of 12-membered ring compound **3b** (1000 mg, 0.967 mmol) and Se powder (791 mg, 10.0 mmol) in 500 mL of freshly distilled ODCB under argon was heated at 180 °C for 2 h. To the solution, 3.5 mL of 0.7 M Na/naphthalene solution (2.45 mmol) in THF was added and the mixture was heated at 180 °C for 4 h. The reaction course was monitored by HPLC equipped with an analytical Buckyprep column (toluene, flow rate = 1 mL/min). The reaction mixture was cooled and directly poured to a short silica gel plug (5 cm × 5 cm) to remove polar materials and obtain a mixture of **3b** and **5b** (toluene/ethyl acetate = 20/1). After removal of the solvents under vacuum, the mixtures were redissolved in toluene and subjected to silica gel chromatography using toluene/ethyl acetate (250/1) to isolate 310 mg of compound **5b** (29%; 37% based on recovered materials) and 50/1 to recover 214 mg of **3b**. Spectral data of **5b**: ^{77}Se NMR (75.5 MHz): 197.0 ppm, with dibenzyl diselenide as an internal reference at 411 ppm; ^{1}H NMR (ODCB-d_4, 300 MHz) δ 6.88 (ddd, J = 0.6, 4.5, 7.2 Hz, 1H), 7.26−7.35 (m, 6H), 7.50 (dt, J = 2.1, 7.8 Hz, 1H), 7.76−7.82 (m, 3H), 8.33 (ddd, J = 0.6, 1.5, 4.5 Hz, 1H), 8.64−8.67 (m, 2H); ^{13}C NMR (ODCB-d_4, 75 MHz) δ 60.46, 72.71, 122.39, 124.87, (126.61−132.56), 132.85, 133.27, 133.80, 135.01, 135.48, 136.21, 136.58, 136.69, 136.97, 137.81, 137.90, 137.95, 137.97, 138.01, 138.08, 138.13, 138.40, 138.71, 138.87, 139.51, 139.62, 139.96, 140.47, 140.70, 140.89, 140.98, 141.38,

141.68, 142.06, 142.42, 144.00, 145.71, 145.93, 145.98, 146.27, 146.65, 146.86, 147.17, 147.26, 147.30, 147.35, 147.44, 147.47, 147.59, 147.82, 147.89, 148.04, 148.11, 148.26, 148.34, 148.54, 148.61, 149.24, 149.29, 150.17, 150.99, 158.86, 166.02, 186.43, 193.29; FT-IR ν (cm^{-1}) (C═O) 1695, 1748. UV−vis ($CHCl_3$, 4.9 × 10^{-5} M) $\lambda_{max}(\epsilon)$ 218 (2.04 × 10^4), 260 (1.35 × 10^4), 318 (5.03 × 10^3), 438 (6.05 × 10^2). HR-FAB MS calcd for $C_{80}H_{15}O_2N_2Se$ ($M + H^+$): 1115.0299; found: 1115.0323.

Synthesis of H_2@4b. To a 100 mg brown and fine powder of compound **4b** wrapped by aluminum foil was applied high pressure of hydrogen gas (760 atm) in autoclave at 190 °C for 8 h. The powder was found to incorporate 100% hydrogen by ^{1}H NMR. Spectral data follow. ^{1}H NMR (ODCB-d_4, 300 MHz) δ −7.36 (s, 2H), 6.72−6.90 (m, 1H), 7.22−7.24 (m, 6H), 7.49−7.54 (m, 1H), 7.78−7.80 (m, 3H), 8.33−8.35 (m, 1H), 8.64−8.66 (m, 2H); ^{13}C NMR (ODCB-d_4, 75 MHz) δ 60.49, 72.68, 122.41, 124.93, (126.45−132.85), 133.60, 133.77, 135.35, 135.67, 136.06, 136.31, 136.75, 137.01, 137.81, 138.03, 138.17, 138.25, 138.36, 138.47, 138.64, 139.66, 139.70, 139.89, 140.26, 140.60, 140.65, 141.12, 141.30, 141.38, 141.76, 141.83, 142.89, 144.11, 145.67, 146.06, 146.10, 146.27, 146.62, 146.76, 146.81, 147.23, 147.35, 147.39, 147.49, 147.57, 147.74, 147.93, 147.96, 148.33, 148.37, 148.44, 148.58, 148.74, 149.36, 149.39, 150.07, 151.45, 159.20, 166.15, 185.97, 192.61; FT-IR ν (cm^{-1}) (C═O) 1697, 1746. APCI MS calcd for $C_{80}H_{16}O_2N_2S$ ($M + H^+$): 1068.1; found: 1068.4. UV−vis ($CHCl_3$, 5.47 × 10^{-5}) $\lambda_{max}(\epsilon)$ 224 (1.26 × 10^4), 258 (1.42 × 10^4), 318 (5.11 × 10^3), 432 (6.73 × 10^2).

Synthesis of H_2@5b. To a 100 mg brown and fine powder of compound **5b** wrapped by aluminum foil was applied high pressure of hydrogen gas (850 atm) in autoclave at 200 °C for 8 h. The powder was found to incorporate 100% hydrogen by ^{1}H NMR. Spectral data follow. ^{77}Se NMR (75.5 MHz): 196.97 ppm, referring to dibenzyl diselenide as internal standard at 411 ppm; ^{1}H NMR (d_4-ODCB, 300 MHz) δ −7.24 (s, 2H), 6.86−6.92 (m, 1H), 7.22−7.34 (m, 6H), 7.47−7.53 (m, 1H), 7.77−7.81 (m, 3H), 8.33−8.35 (m, 1H), 8.63−8.65 (m, 2H); ^{13}C NMR (d_4-ODCB, 75 MHz) δ 60.47, 72.69, 122.39, 124.90, (126.27−132.85), 133.57, 133.80, 135.20, 135.68, 136.27, 136.60, 136.71, 137.06, 137.90, 137.97, 138.00, 138.09, 138.10, 138.15, 138.19, 138.46, 138.58, 139.00, 139.58, 139.70, 140.01, 140.59, 140.83, 140.92, 141.12, 141.29, 141.68, 141.81, 142.12, 142.54, 144.02, 145.65, 145.95, 146.22, 146.72, 146.93, 147.23, 147.33, 147.36, 147.39, 147.46, 147.52, 147.64, 147.89, 147.97, 148.09, 148.17, 148.26, 148.42, 148.56, 148.66, 149.26, 150.14, 151.13, 158.91, 166.05, 186.47, 193.27; FT-IR ν (cm^{-1}) (C═O) 1696, 1747. APCI-MS calcd for $C_{80}H_{16}O_2N_2Se$ (M^+): 1116.04; found: 1116.6. UV−vis ($CHCl_3$, 6.48 × 10^{-5} M) $\lambda_{max}(\epsilon)$ 220 (1.64 × 10^4), 260 (1.37 × 10^4), 318 (5.10 × 10^3), 438 (6.07 × 10^2).

Synthesis of Compound 7a. A solution of compound **3a** (209 mg, 0.202 mmol) and *p*-tolylhydrazine•HCl (35.9 mg, 0.226 mmol) in 15 mL ODCB/THF (v/v 2/1) was heated 65 °C under argon. The resulting mixture was treated with pyridine (0.09 mL, 1.226 mmol), stirred at 65 °C for 4 h and monitored by HPLC. The color of the mixture slowly turned dark black. Compound **7a** appeared at retention time (t_R) of 4.6 min (Buckyprep analytical column, flow rate 1 mL/min, toluene). When the starting material **3a** was completely consumed (t_R = 7.2 min), the reaction mixture was evacuated to remove THF and then poured to a silica gel column to separate from polar materials. A dark-brown solution of **7a** was collected using toluene/ethyl acetate (20/1) as eluent. After removal of solvent under vacuum, 180 mg (77%) **7a** was isolated as a black solid. Spectral data follow. ^{1}H NMR (CS_2/$CDCl_3$ = 1:5, 300 MHz) δ 2.39 (s, 3H), 4.77 (d, J = 20.2 Hz, 1H), 5.43 (d, J = 19.8 Hz, 1H), 6.88−7.33 (m, 11H), 7.55 (d, J = 8.7 Hz, 2H), 7.65 (dd, J = 1.6, 7.9 Hz, 1H), 7.69 (dd, J = 1.6, 7.9 Hz, 1H), 7.76 (d, J = 7.9 Hz, 1H), 7.88 (dt, J = 1.6, 7.9 Hz, 1H), 8.60 (d, J = 4.4 Hz, 1H), 13.62 (s, 1H). ^{13}C NMR (CS_2/$CDCl_3$ = 1:5, 99.5 MHz) δ 23.16, 44.12, 53.12, 76.00, 116.28, 123.41, 123.62, 127.14, 127.24, 127.29, 127.62, 128.04, 128.17, 128.65, 128.81, 129.13, 129.50, 130.04, 130.11, 130.29, 130.65, 131.20, 131.22, 131.83, 133.62, 135.10, 135.46, 136.04, 136.12, 136.51, 136.60, 137.39, 137.44, 137.62, 137.75, 138.17, 138.28, 138.78, 140.48, 140.60, 140.92, 141.65, 141.92, 142.69, 142.76, 143.04, 143.10, 143.45, 142.97, 143.99, 144.69, 145.51, 145.63, 145.75, 146.45, 146.75, 146.88, 147.34, 147.41, 147.47, 147.62, 147.89, 147.93, 148.00, 148.08, 148.26, 148.28, 148.59, 148.68, 148.75, 148.94, 149.25, 149.47, 149.57, 149.69, 149.90, 150.87, 152.11, 153.73, 163.20, 167.71, 183.89, 193.75. HRMS (FAB-positive mode) calcd for $C_{87}H_{25}O_2N_4$ ($M + H^+$): 1157.1978; found: 1157.2004. FT-IR ν (KBr, cm^{-1}) 1531, 1686. UV−vis ($CHCl_3$, 5.01 × 10^{-5} M) $\lambda_{max}(\epsilon)$ 258 (1.26 × 10^4), 328 (4.70 × 10^3), 444 (2.05 × 10^3), 544 (1.31 × 10^3), 630 (6.09 × 10^2), 696 (5.69 × 10^2).

Synthesis of Compound 7b. To a solution of compound **3b** (204 mg, 0.197 mmol) and *p*-tolylhydrazine•HCl (38.9 mg, 0.217 mmol) in 15 mL ODCB/THF (v/v 2/1) under argon was added pyridine (0.1 mL 1.226 mmol). The resulting mixture was stirred at 65 °C for 4 h and monitored by HPLC. The color of the mixture slowly turned dark black. Compound **7b** appeared at t_R = 4.3 min (Buckyprep analytical column, flow rate 1 mL/min, toluene). When the starting material **3b** was completely reacted (t_R = 6.1 min), the reaction mixture was evacuated to remove THF and then poured to a silica gel column to separate from polar materials. A dark-brown solution of **7b** was collected using toluene/ethyl acetate (20/1) as eluent. After removal of solvent under vacuum, 165 mg (72%) of **7b** was isolated as a black solid. Spectral data follow. ^{1}H NMR ($CDCl_3$, 300 MHz) δ 2.47 (s, 3H), 4.85 (d, J = 20.4 Hz, 1H), 5.70 (d, J = 20.4 Hz, 1H), 7.07−7.37 (m, 11H), 7.50 (d, J = 8.4 Hz, 2H), 7.61−7.63 (br, 1H), 7.78 (dt, J = 2.1, 8.1 Hz, 1H), 7.83−7.86 (m, 1H), 7.90−7.93 (m, 2H), 8.58−8.60 (m, 1H). ^{13}C NMR ($CDCl_3$, 75.5 MHz) δ 21.12, 44.23, 60.66, 72.93, 115.01, 122.40, 123.94, 126.23, 127.07, 127.19, 127.40, 128.07, 128.79, 128.88, 129.41, 129.72, 130.25, 130.49, 130.99, 131.15, 131.39, 132.60, 134.45, 134.58, 135.62, 135.91, 135.92, 136.52, 136.55, 136.94, 137.04, 137.13, 137.87, 138.16, 138.42, 138.44, 139.88, 140.29, 140.38, 141.25, 141.39, 143.55, 142.27, 143.00, 143.47, 143.53, 143.59, 143.88, 143.94, 144.79, 145.27, 145.34, 146.13, 146.40, 146.98, 147.02, 147.27, 147.37, 147.50, 147.56, 147.66, 147.72, 148.20, 148.39, 148.81, 148.85, 149.14, 149.27, 149.58, 149.78, 150.47, 151.45, 154.99, 165.08, 165.23, 185.59, 196.69. HRMS (FAB-positive mode) calcd for $C_{87}H_{25}O_2N_4$ ($M + H^+$): 1157.1978; found: 1157.1981. FT-IR ν (KBr, cm^{-1}) 1537, 1681. UV−vis ($CHCl_3$, 6.48 × 10^{-5} M) $\lambda_{max}(\epsilon)$258 (1.26 × 10^4), 328 (4.60 × 10^3), 444 (2.04 × 10^3), 544 (1.33 × 10^3), 628 (6.54 × 10^2), 692 (6.06 × 10^2).

Synthesis of Compound H_2@7a. To a 65 mg (0.056 mmol) brown and fine powder of compound **7a** wrapped by aluminum foil was applied high pressure of hydrogen gas (660 atm) in autoclave at 180 °C for 5 h. The powder was found to incorporate 69% hydrogen by ^{1}H NMR. Spectral data follow. ^{1}H NMR (CS_2/$CDCl_3$ = 1:5, 300 MHz) δ −7.13 (1.38H), 2.47 (s, 3H), 4.85 (d, J = 20.4 Hz, 1H), 5.70 (d, J = 20.4 Hz, 1H), 7.09−7.40 (m, 11H), 7.49−7.52 (m, 2H), 7.61−7.63 (m, 1H), 7.75−7.80 (m, 1H), 7.83−7.86 (m, 1H), 7.61−7.63 (m, 1H), 8.58−8.60 (m, 1H), 13.98 (s, 1H). APCI-MS (positive mode) calcd for $C_{87}H_{27}O_2N_4$ ($M + H^+$): 1159.2; found: 1159.8.

Synthesis of Compound H_2@7b. To a 55 mg (0.048 mmol) brown and fine powder of compound **7b** wrapped by aluminum foil was applied high pressure of hydrogen gas (660 atm) in autoclave at 180 °C for 6 h. The powder was found to incorporate 62% hydrogen by ^{1}H NMR. Spectral data follow. ^{1}H NMR ($CDCl_3$, 300 MHz) δ −7.15 (s, 1.24H), 2.40 (s, 3H), 4.87 (d, J = 20.0 Hz, 1H), 5.55 (d, J = 20.0 Hz, 1H), 6.88−7.40 (m, 11H), 6.88−7.40 (m, 2H), 7.70−7.77 (m, 3H), 7.88−7.91 (m, 1H), 8.65−8.68 (m, 1H) 13.63 (s, 1H). APCI-MS (positive mode) calcd for $C_{87}H_{27}O_2N_4$ ($M + H^+$): 1159.2; found: 1159.2.

Kinetic Study of H_2 Release Measurement. For an example, the rate of hydrogen release was measured at four temperatures, 120, 130, 140, and 150 °C. The NMR sample was prepared by

dissolving 4 mg of H_2@**4b** in 0.5 mL of ODCB-d_4 and treated with FPT (freeze−pump−thaw) process until no gas evolution occurred. NMR measurement was conducted at appropriate time interval at each temperature and hydrogen content was calculated and plotted against time. The rate constant was extracted from the fitted exponential decay plot.

Acknowledgment. This work was supported by a Grant-in-Aid for Scientific Research (C) (No. 18550033) and Young Scientists (A) (No. 16681008) from the Ministry of Education, Culture, Sports, Science, and Technology, Japan.

Supporting Information Available: ^{1}H and ^{13}C NMR spectral data of new compounds. Cartesian coordinates of optimized structure and transition state structure. This material is available free of charge via the Internet at http://pubs.acs.org.

JO070790W